YMTHE, Volume *28*

Supplemental Information

Non-viral Gene Therapy for Stargardt Disease with ECO/*pRHO-ABCA4* Self-Assembled Nanoparticles

Da Sun, Rebecca M. Schur, Avery E. Sears, Song-Qi Gao, Amita Vaidya, Wenyu Sun, Akiko Maeda, Timothy Kern, Krzysztof Palczewski, and Zheng-Rong Lu

Supplementary Results

Cytotoxicity of ECO/*pDNA* nanoparticles

The toxicity of the ECO/*pCMV-ABCA4* nanoparticles and control Lipofectamine/*pCMV-ABCA4* nanoparticles were evaluated in the ARPE-19 cell line (human retinal pigmented epithelium) using the MTT assay. Cell viability was evaluated 48 h after transfection with nanoparticles (**Figure S1A)**. The ECO/*pCMV-ABCA4* nanoparticles demonstrated a more than 85% cell viability in comparison to the Lipo/*pCMV-ABCA4* nanoparticles, which had a cell viability of less than 40%. The Cell viability of ECO/*pCMV-ABCA4* nanoparticles with different *pCMV-ABCA4* concentrations was also tested in ARPE-19 cells 48 h after transfection using a CCK-8 assay (**Figure S1B**). A dose dependent cell viability was observed.

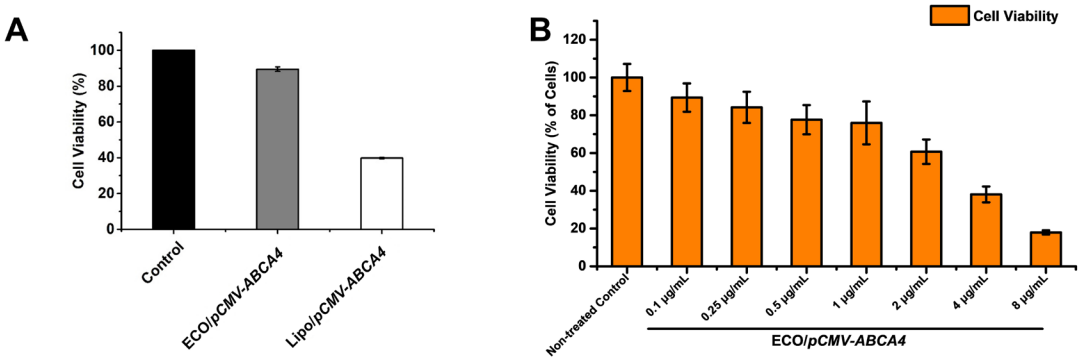

Figure S1. Cell viability of ECO/*pCMV-ABCA4* nanoparticles in ARPE-19 cells 48 h after transfection, demonstrated by **(A)** an MTT assay, with non-treated ARPE-19 cells and lipofectamine/*pCMV-ABCA4* nanoparticles as controls (The concentration of *pCMV-ABCA4* was 1 µg/mL in the culture media) and **(B)** CCK-8 assay, with different *pCMV-ABCA4* concentrations.

Specific Gene Expression induced by RHO promoter

The flow cytometry histograms of *in vitro* transfection of ECO and Lipofectamine

nanoparticles in ARPE-19 cells were shown in **Figure S2**, which were the corresponding profiles of what was shown in **Figure 2B**.

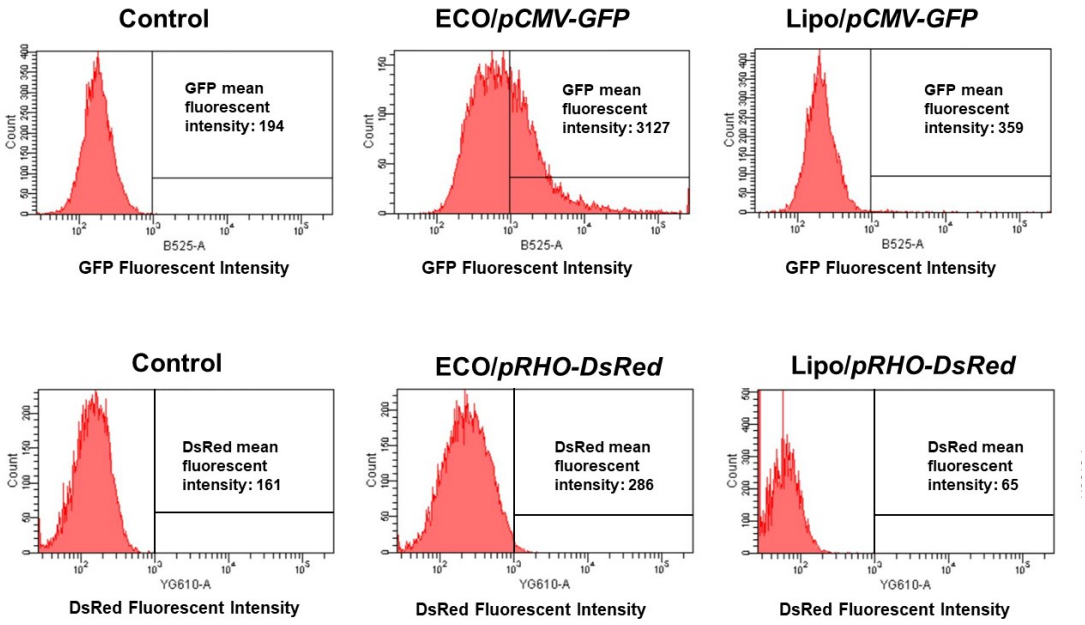

Figure S2. Flow cytometry histograms of *in vitro* transfection of ECO and Lipofectamine nanoparticles in ARPE-19 cells using reporter plasmids. Flow cytometry was performed 48 h post transfection. Mean fluorescent intensities were listed in the histograms.

Synthesis of therapeutic plasmid (*pRHO-ABCA4*)

The photoreceptor-specific *pRHO-ABCA4* plasmid was constructed using molecular cloning to insert the *ABCA4* gene into the backbone of the DsRed reporter plasmid containing the bovine rhodopsin promoter region (**Figure S3**). The *ABCA4* gene was amplified by PCR using the Q5 DNA polymerase enzyme for high fidelity amplification of the large (6.8 kb) gene product. Primers were designed with 4 regions (**Figure S4**):

1. A three-nucleotide buffer region at the 5'-end to aid in the binding of the restriction endonucleases to the amplicon.
2. The restriction site to be digested, matching the insertion site of the vector at *AgeI* for the forward primer and *NotI* for the reverse primer. Digestion at

these restriction sites generates incompatible sticky ends to ensure gene insertion in the proper direction.

3. A 21-22 nucleotide overlap with the gene from the start or stop codon.

PCR amplification was verified using gel electrophoresis of the full reaction product. As expected, the size of the amplicon (6.8 kb) matched the size of the *ABCA4* gene isolated by a restriction digest at its flanking sites of NotI and NheI (**Figure S4E**). Following PCR amplification, the *ABCA4* amplicon and the p*RHO-DsRed* plasmid were digested at the AgeI and NotI restriction sites to generate the sticky ends necessary for ligation. Agarose gel electrophoresis verified that *ABCA4* retained its size without extraneous digestion of the gene. Furthermore, the gel result demonstrated successful removal of the *DsRed* gene (0.7 kb) from the plasmid backbone with the RHO promoter site (5.4 kb).

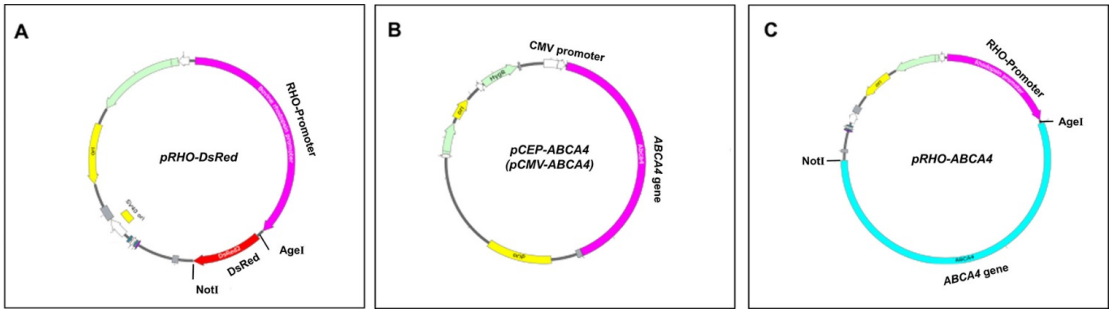

Figure S3. Plasmid construction strategy for *pRHO-ABCA4*. (A) *pRHO-DsRed* vector. *DsRed* is excised from the *pRHO-DsRed* plasmid at the *AgeI* and *NotI* restriction sites, leaving the *pRHO* backbone with sticky ends at *AgeI* and *NotI* at the 3'- and 5'-ends, respectively. (B) PCR amplification of the *ABCA4* cDNA gene product from the *pCEP4-ABCA4 (pCMV-ABCA4)* plasmid. PCR primers are designed to add the AgeI and *NotI* restriction sites to the *ABCA4* gene, and the product was digested at those sites to generate compatible sticky ends with the *pRHO* vector. (C) Final *pRHO-ABCA4* plasmid following ligation of the *pRHO* vector with the *ABCA4* gene insert is shown.

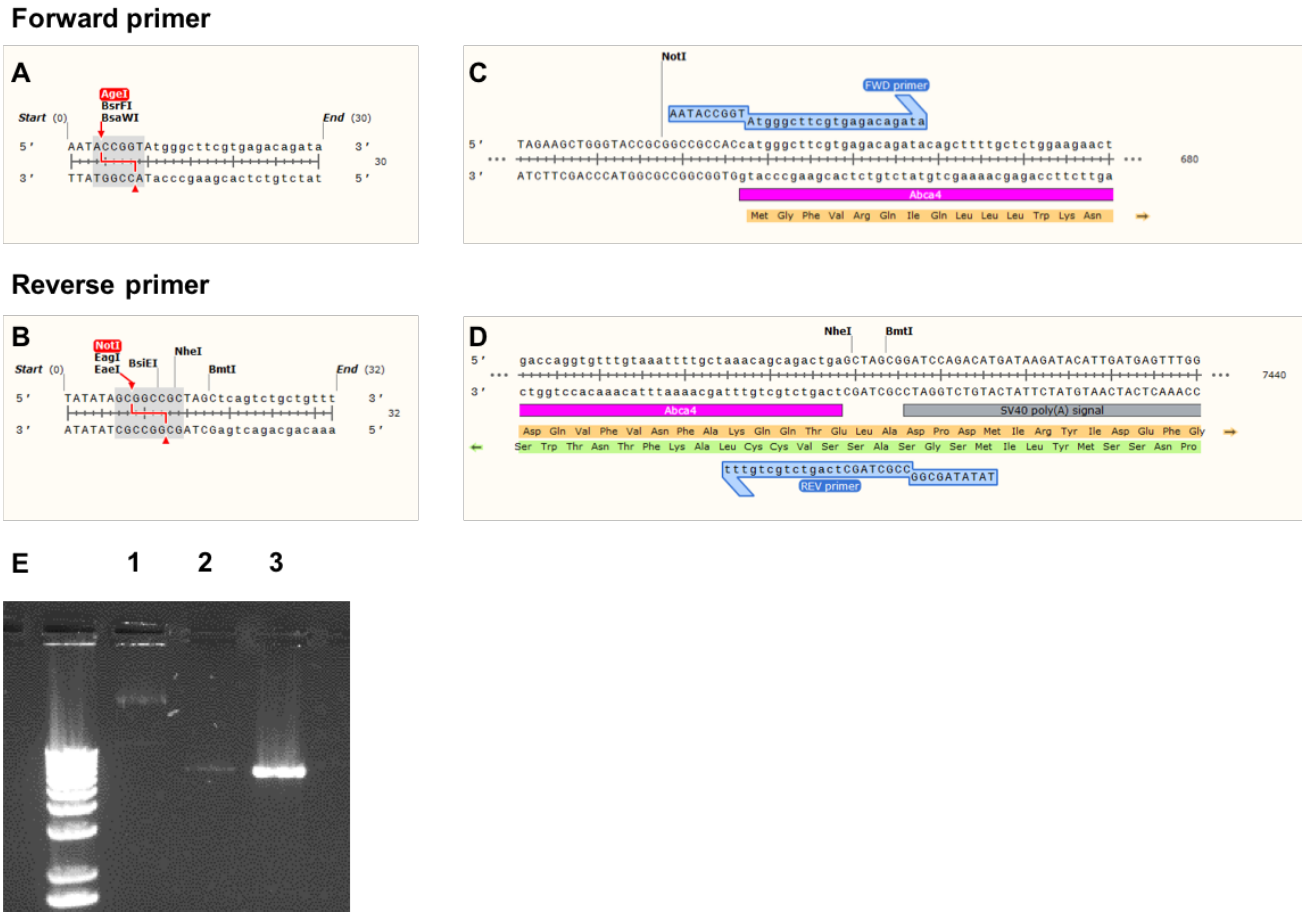

Figure S4. Primer design for PCR amplification of *ABCA4*. (A-B) Oligonucleotide sequences for the forward and reverse primers demonstrating the insertion of restriction sites *AgeI* and *NotI,* respectively. (C-D) Overlap of forward and reverse sequences with *pCEP4-ABCA4 (pCMV-ABCA4)* for amplification of the *ABCA4* gene between the stop and end codons. (E) Agarose gel electrophoresis of PCR amplification of the *ABCA4* gene from the *pCEP4-ABCA4 (pCMV-ABCA4)* plasmid. **Lane 1:** circular *pCEP4-ABCA4 (pCMV-ABCA4)* plasmid; **Lane 2:** Restriction digestion of *ABCA4* excised from the *pCEP4-ABCA4 (pCMV-ABCA4)* plasmid at the NotI and NheI restriction sites; **Lane 3**: PCR product of the amplified *ABCA4* gene by the high fidelity Q5 DNA polymerase enzyme. Size of the PCR amplicon is consistent with the expected size of the gene product.

Confirmation of *ABCA4* cDNA by sequencing

Plasmid of *pRHO-ABCA4* was purified by Qiagen miniPrep kit and used for sequencing template. Nine sequencing primers were designed according to human *ABCA4* (Ref NM_000350) with around 700 bp spanning to cover the whole 6.8 kb. Detailed primer information is listed in **Table. S1**. The reading results covered *ABCA4* full length and BLAST to NM_000350 showed sequences identical except 3 polymorphisms at position 141 A>G, 5175 G>A and 6069 T>C. All 3 polymorphisms had no amino acid coding change involved.

Table S1. Sequencing primers for *ABCA4*

Primer	Sequence	Location
F1	AGCTCAAGCTTCGAATTCTGC	upstream of *ABCA4*
F2	ATGCCAACGTGGACTTCTTC	734-753
F3	CGCCTGGTCAATCAATACCT	1530-1550
F4	TCTACCTGCCACACATCCTG	2314-2334
F5	AAAGGAAAGTCCCAGGAGGA	3090-3110
F6	GAAGGTCACGGAGGATTCTG	3821-3841
F7	ACCTGACGGACAGGAACATC	4570-4590
F8	GATGTACCCAGCATCCTTCC	5330-5350
F9	CTGCTCACAGGACGAGAACA	6075-6095

A2E accumulations in untreated *Abca4*$^{-/-}$ mice and the synthesis of A2E standard

A2E standard was purified with HPLC, collected at the retention time of 14.9 min (**Figure S5A**). The mass of A2E was confirmed by MALDI-TOF mass spectrometry with a molecular weight of 592.47 (**Figure S5B**). To understand STGD disease progression in the orthologous mouse model (*Abca4*$^{-/-}$ mice), the A2E levels in untreated mice were analyzed at different ages. Mice were euthanized at ages of 2, 3, 4 and 5 months. A2E was extracted from the eye samples. As demonstrated in **Figure S5C and D**, A2E was identified in the eye extractions and confirmed by comparing the UV spectra with A2E standard. Unlike patients who exhibit atrophy in the macular region, however, the pigmented orthologous mouse model did not undergo retinal degeneration. While photoreceptor degeneration was limited, lipofuscin accumulation in *Abca4*$^{-/-}$ mice was consistently elevated as early as 3 months of age, demonstrated by HPLC analysis (**Figure S5E**).

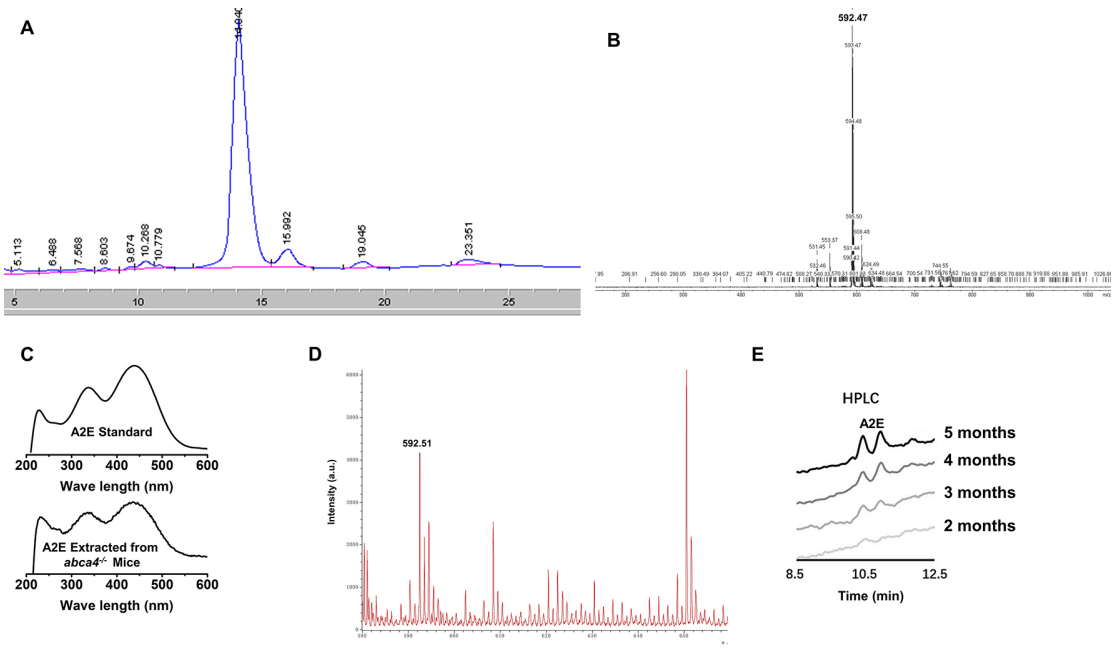

Figure S5. (A) HPLC analysis of A2E standard with a retention time of 14.9 min. (B)

MALDI-TOF Mass spectrum of A2E. (Mw (A2E) =592.47) **(**C) UV spectra of synthesized A2E standard and A2E extracted from *Abca4*$^{-/-}$ mice. (D) ESI Mass spectrum of an eye extraction and A2E could be observed with a molecular weight of 592.51. (E) A2E accumulations in untreated *Abca4*$^{-/-}$ mice with different ages analyzed by HPLC.

Safety of gene therapy using ECO*/pABCA4* nanoparticles

The safety of ECO/*pABCA4* nanoparticles was evaluated based on the retinal morphology from optical coherence tomography (OCT) and retinal function from Electroretinography (ERG). OCT images of retinal structure (**Figure S6A**) indicated severe retinal detachments in around 10 % of mice in the treatment group due to subretinal injections, and these mice were excluded from ERG analysis. With the contralateral uninjected eye as control, ERGs recorded 7 and 30 days (**Figure S6B**) after treatment indicated moderate loss of visual function in some injected eyes, represented by decreased scotopic a- and b- wave amplitudes in some groups. Photopic wave amplitudes did not change significantly compared to the no injection controls. There was no significant difference amongst all subretinal injected groups in ERG wave intensities.

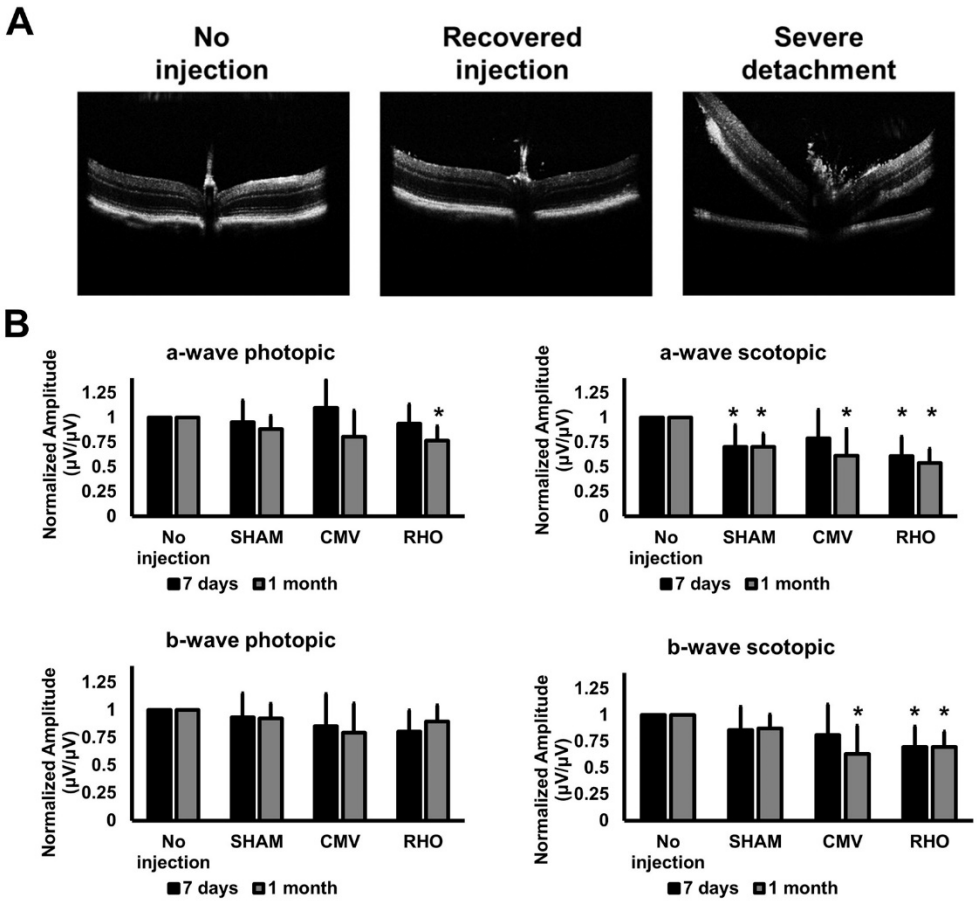

Figure S6. Safety evaluation of ECO/*pABCA4* nanoparticle based gene replacement therapy (GRT) in wild type 129S1/SvImJ mice. (A) Representative OCT images of (left) a healthy, uninjected eye, (middle) a treated eye following recovery from subretinal injection, and (right) a severely detached retina in a treated eye that did not recover from the injection. (B) ERG a-wave and b-wave amplitudes analyzed 7 and 30 days after injection with PBS (sham), ECO/*pCMV-ABCA4*, or ECO/*pRHO-ABCA4* in one eye. Amplitudes were normalized to the contralateral uninjected eye. Error bars = ± sd (n =4 * $P< 0.05$ relative to no injection control. Statistical analysis was conducted with ANOVA.).